

## Field studies of the natural and built environments using large mobile shakers

K.H. Stokoe, II, S. Hwang, B.R. Cox, & F.Y. Menq,

*Department of Civil, Architectural and Environmental Engineering, University of Texas at Austin, Austin, Texas, USA*

J.N. Roberts,

*Geosyntec Consultants, Inc., Columbia, Maryland, USA*

K. Park,

*Fugro USA Land, Inc., Houston, Texas USA*

**ABSTRACT:** An overview of some field studies that are now possible due to the development of five large mobile shakers and associated field support vehicles is presented. Development of this equipment has been funded by the U.S. National Science Foundation. Characteristics of the five mobile shakers are briefly reviewed. Four types of testing involving the mobile shakers are discussed. Examples of noninvasive shear-wave velocity ( $V_s$ ) profiling using surface-wave methods with active sources or combined with active and passive sources over depths from 10 to 1000 m are presented. Deep downhole seismic profiling with controlled-waveform compression and shear waves to  $> 400$  m is presented. Two in-situ parametric studies are discussed. The first study involves evaluating the shear-modulus nonlinearity of a cemented alluvium. The second study involves evaluating pore-water pressure generation in loose saturated sand. Finally, the effects of dynamic and slow-cyclic loading on soil-foundation-structure interaction using scaled structural systems are presented.

### 1 INTRODUCTION

The primary objective of this theme paper is to present an overview of some types of field studies that are now possible because of the development of large mobile shakers. Development of these mobile shakers and associated field equipment has been funded by the U.S. National Science Foundation (NSF), initially under the Network for Earthquake Engineering Simulation (NEES) program from 2000 to 2014 and now under the Natural Hazards Engineering Research Infrastructure (NHERI) program from 2016 to 2020. The primary applications that are presented herein deal with earthquake engineering studies in the geotechnical and soil-structure interaction areas. In each application, detailed background information about the testing technique is not presented but is simply cited using references so that recent example results can be highlighted and used to illustrate new directions in field testing. It is also important to note that the U.S. National Science Foundation has created NHERI@UTexas as part of a larger, shared-use infrastructure which is available to researchers in the U.S. and other cooperating researchers around the world. (NHERI, 2017). As an example, one large mobile shaker from NHERI@UTexas was used in the Christchurch, NZ area on a cooperative, field liquefaction study involving researchers from both countries (Stokoe et al., 2014).

The theme paper is organized as follows. First, a brief overview of the large mobile shakers is presented. The remainder of the paper covers applications of this equipment. The applications are: (1) noninvasive shear-wave velocity ( $V_s$ ) profiling using surface-wave methods, (2) deep downhole testing using compression (P) and shear (S) waves, (3) parametric studies in which the effects of stress state on wave velocities and strain amplitude on shear-modulus nonlinearity can be evaluated, (4) performance of in-situ liquefaction testing to evaluate parameters such as the threshold strain at which pore-water pressure begins to be generated and the effect of number of loading cycles, and (5) the effects of soil-foundation-structure interaction under dynamic and slow-cyclic loading and static loading to failure using scaled structural systems in the field.

## 2 OVERVIEW OF THE NHERI@UTEXAS EQUIPMENT FACILITY

The NHERI@UTexas equipment facility can be subdivided into six components. The first component is the five, large, hydraulically-controlled shakers that can be used as mobile, wide-band dynamic sources for excitation of geotechnical and structural systems. These mobile shakers offer a wide range in force and frequency generation capabilities. For easy identification of the shakers, they have been given the following names: (1) T-Rex, (2) Liquidator, (3) Raptor, (4) Rattler, and (5) Thumper (see photographs in Figure 1a through 1e, respectively). T-Rex is capable of generating large dynamic forces in any of three directions (vertical, horizontal in-line, and horizontal cross-line). The second large shaker, Liquidator, is a custom-built, shaker that was designed specifically for low-frequency, large-motion operation in either the vertical mode (compression or surface wave generation) or the cross-line horizontal (shear) mode. There is no other shaker like Liquidator in the world. The two, intermediate-sized shakers, based on force-generation characteristics and vehicle weight, are Raptor and Rattler. Raptor is called a compression-wave (P-wave) shaker and Rattler is called a shear-wave (S-wave) shaker in the geophysical exploration community. The smallest shaker is called Thumper. Thumper has a moderate force output, which makes it ideal for testing in urban areas. The theoretical vertical and horizontal frequency-force outputs are shown in Figures 2a and 2b, respectively. This set of five mobile shakers separates NHERI@UTexas from any other university facility.

The mobile shakers also require some field support vehicles. T-Rex, Liquidator, and Rattler must be transported to and from test sites on the 26-wheel, tractor-trailer rig, called the Big Rig, shown in Figure 1f. The large size of the tractor-trailer rig is required because both T-Rex and Liquidator create “over-load” situations. Also, due to regulations in some states, Raptor has to be transported with the tractor-trailer rig. Another field-support vehicle is a supply truck (see Figure 1g) that carries diesel fuel for the four largest shakers and also carries spare parts and provides a working platform for maintenance in the field. The third support vehicle is a 2.4 m by 4.8 m instrumentation trailer with storage space, air-conditioned work space, waveform analyzers and computers, and electrical power (see Figures 1g, 1h and 1i, respectively). Both T-Rex and Liquidator also have the capability of pushing CPT equipment (see Figure 1j) as well as pushing other sensors into the ground to create embedded instrumentation arrays. Additional information on the NHERI@UTexas experimental facility can be found in Stokoe et al., 2017a.

## 3 NONINVASIVE $V_s$ PROFILING USING SURFACE-WAVE METHODS WITH ACTIVE SOURCES OR COMBINED ACTIVE AND PASSIVE SOURCES

Noninvasive  $V_s$  profiling using the active-source, Spectral-Analysis-of-Surface-Waves (SASW) method has been performed for years before T-Rex and Liquidator were conceived and developed. This work was initially performed using intermediate-sized shakers like Raptor. At that time, the mobile shaker was rented from an exploration geophysical contractor and a specially modified, frequency-control system had to be used in place of the standard waveform control system. The modified waveform control system allowed downward frequency sweeps with selectable frequency ranges, frequency steps and durations at each step to be controlled by an independent spectrum analyzer that was also used to collect the signals from multiple geophones in the surface array (Stokoe et al., 2004). This combination of simultaneously controlling the exciting and recording with the same spectrum analyzer permitted excellent signal filtering and high-fidelity recording. Today, all NHERI@UTexas mobile shakers operate with this advanced frequency-control system. Three different projects using the active-source SASW method are presented to illustrate the applications and findings. Background information covering the SASW method is presented in Stokoe et al., 2017b. In addition, a fourth surface-wave project that involved using combined active and passive sources is presented. Background information covering the combined active and passive surface-wave methods is presented in Teague et al., 2018.

### 3.1 *Shallow, active-source, SASW testing of a dam spillway on rock*

The first project involves an investigation of a dam spillway on rock. The purpose of these measurements was to determine noninvasively if any subsurface weaknesses existed within about 8 m



Figure 1. Photographs of the five mobile shakers, tractor-trailer rig, field supply truck, instrumentation trailer with air-conditioned work space and instrumentation, and pushing capabilities on the back of T-Rex and Liquidator that are available at NHERI@UTexas (Stokoe et al., 2017a).

of the spillway surface in designated areas of concern. In this case of concrete over rock, the wave velocities in the material being sampled are about ten times higher than the wave velocities at soil sites. Therefore, the frequencies of surface waves required at “rock” sites to profile this material are also about 10 times higher. As a result, transient impacts with small hand-held hammers were used to generate frequencies in the range of about 400 to 8,000 Hz, and Thumper was used to sinusoidally shake in a downward sweep over frequencies from 400 to 20 Hz. A photograph of

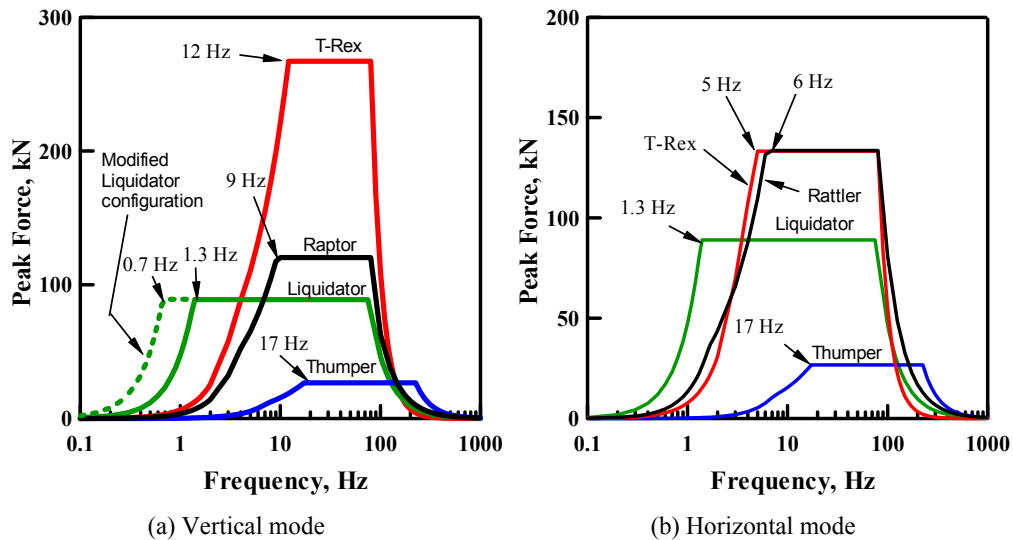


Figure 2. Theoretical force outputs of the five mobile shakers at NHERI@UTexas (Stokoe et. al, 2017a).

Thumper in one of the spillway areas is shown in Figure 3a. In this case, SASW testing was being performed using surface waves propagating in the west-to-east direction which is perpendicular to the direction of water flowing down the spillway. However, SASW testing was also performed at multiple locations parallel to the direction of water flow (north to south). In these cases, Thumper was positioned at the same relative location as shown in Figure 3a, but the SASW array was located in the north-to-south direction along each spillway. A  $V_s$  profile from one set of tests along a spillway centerline is presented in Figure 3b. In this profile, the concrete has a slightly higher shear wave velocity than the rock immediately below the concrete. However, this upper rock layer has a  $V_s$  value of very good rock, and the rock below has the highest  $V_s$  value in the profile; hence, no zone of weakness in this portion of the spillway. It is also important to note that: (1) the transient hammer blows only permitted investigation of about the top 2.5 m of the spillway, (2) the sinusoidal sweep with Thumper generated the lower frequencies required to profile to a depth of 10 m, and (3) no larger-hammer impacts or transient drop-weight impacts on rock could generate the lower frequencies that were generated using Thumper.

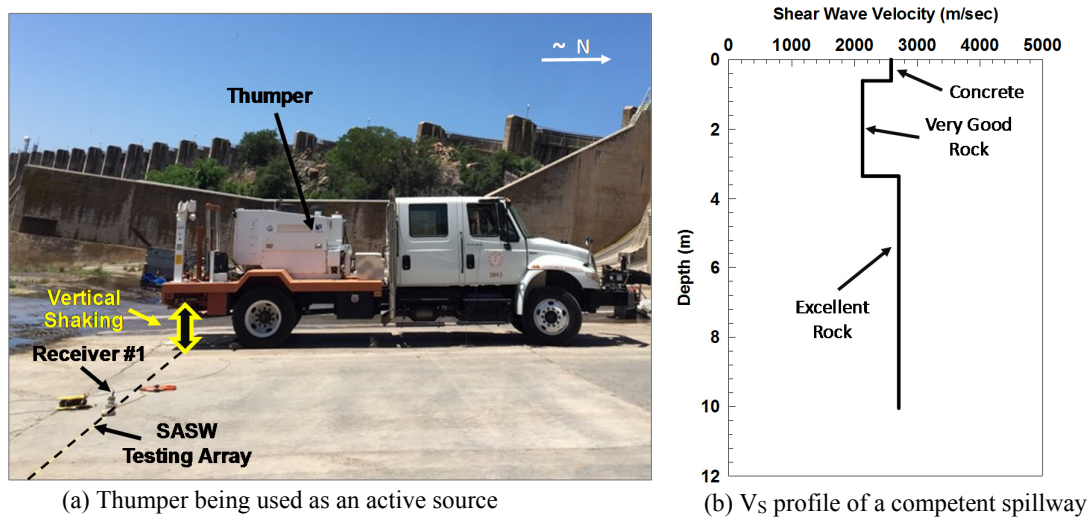


Figure 3. SASW testing of dam spillways composed of concrete over rock to investigate potential zones of weaknesses in the rock.

### 3.2 Deep ( $> 300$ m) $V_S$ profiling on top of Yucca Mountain using Liquidator as the source

As part of studies to characterize a potential geologic repository for high-level radioactive waste and spent nuclear fuel in the United States, a comprehensive program of deep seismic profiling was conducted around Yucca Mountain, Nevada to evaluate the  $V_S$  structure of the mountain. The resulting  $V_S$  data were used as input into the development of ground motions for the preclosure seismic design of the repository and for postclosure performance assessment. The SASW method was employed in the deep profiling which was defined as profiling to depths of 300 to 450 m. One key element in successfully performing the deep  $V_S$  profiling at Yucca Mountain was the shear wave velocities of the rock that was composed of layers of tuffs with  $V_S$  values generally above 800 m/s at depths greater than 80 m. The second key element was the active source, Liquidator (see Figure 4a), which could generate frequencies as low as 1 Hz. Typically, it was only possible to test one site per day due to the time required to deploy receivers over large distances up to 1000 m (see Figure 4b), combined with the extended duration of the stepped-sine, downward sweep at low frequencies which required more than 45 minutes of constant shaking. Nevertheless, deep profiling was performed at a total of 17 sites.

Once the 17  $V_S$  profiles were determined, it became clear that the  $V_S$  profiles could be subdivided into two groups. The following statistical data were determined for each group: (1) median, 16<sup>th</sup> and 84<sup>th</sup> percentile profiles of  $V_S$ , and (2) the coefficient of variation (COV) which is equal to one standard deviation divided by the mean of the  $V_S$  values at each depth. The data sets for Groups 1 and 2 are presented in Figures 5a and 5b, respectively. The Group-1  $V_S$  profiles in Figure 5a have a smaller gradient in the median  $V_S$  profile than the Group-2  $V_S$  profiles. It is also interesting to note that the  $V_S$  values measured by SASW testing in a tunnel at the proposed repository level (depth about 300 m) below the general locations of the Group-1 surface measurements agree well with the Group-1  $V_S$  values at the 300-m depth. The Group-2  $V_S$  profiles, presented in Figure 5b, were located in a general area where the proposed repository level was shallower (about 260 m). The Group-2  $V_S$  profiles exhibit a larger gradient and higher  $V_S$  values around the repository level compared to the Group-1 profiles. Also, similar to the Group-1 measurements, the  $V_S$  values measured in the tunnel at the proposed repository level (depth of about 260 m) agree well with the Group-2  $V_S$  values at the 260-m depth.

Finally, it is also interesting to note that low COV values were evaluated over much of the profile for Groups 1 and 2, generally less than 0.13. The COV values increased to around 0.20 at depth in both groups. The increased COV values were not at the same depths in both velocity groups but seemed to be related more to variations in the depths of the layer boundaries with significant contrasting velocities. This finding is often observed at geotechnical sites spread over areas of 10's of square kilometers with profiling depths of 100 to 200 meters.

### 3.3 Very-deep ( $> 500$ m) $V_S$ profiling at a greenfield site using Liquidator in a modified mode

At times when performing deep  $V_S$  profiling with Liquidator, the project would have benefited from even deeper profiling. Therefore, over the past six years, personnel of NHERI@UTexas have worked to increase the peak force level at frequencies below about 1.3 Hz. This desired

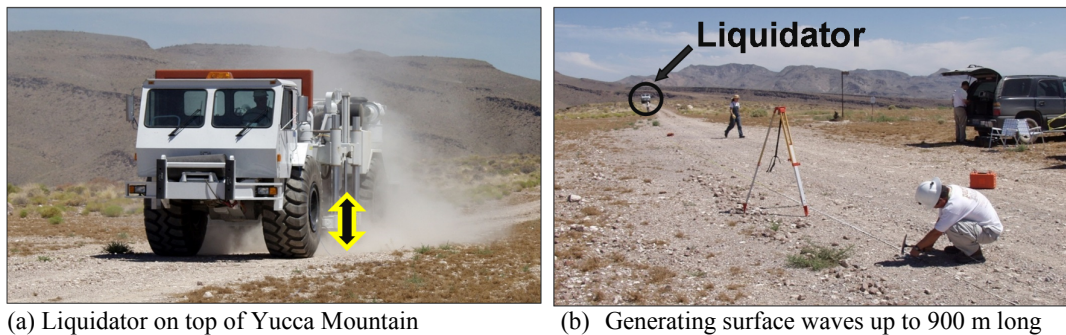
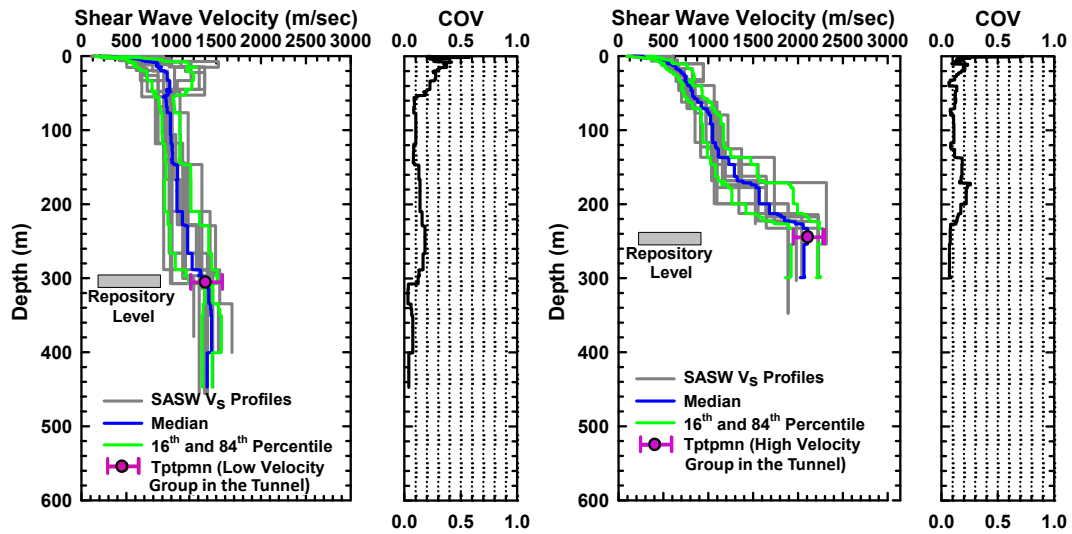


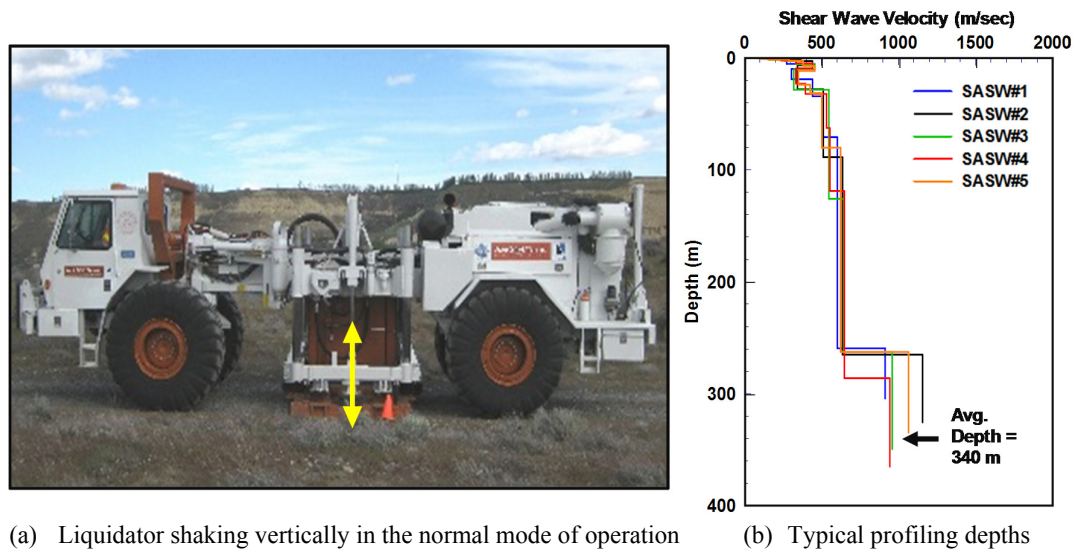
Figure 4. Deep SASW profiling on top of Yucca Mountain, NV using Liquidator as the low-frequency, active source to generate surface wavelengths ranging from about 15- to 900-m long.



(a) Group-1: Nine softer sites with median and  $\pm \sigma$   $V_S$  profiles and comparison of these profiles with  $V_S$  values measured in a tunnel beneath the surface testing locations  
 (b) Group-2: Eight stiffer sites with median and  $\pm \sigma$   $V_S$  profiles and comparison of these profiles with  $V_S$  values measured in a tunnel beneath the surface testing locations

Figure 5. Comparison of the Group-1 (“softer”) and Group-2 (“stiffer”)  $V_S$  profiles in two different areas of Yucca Mountain, and comparisons of these two groups of  $V_S$  profiles with  $V_S$  values measured in a tunnel at the proposed repository levels below each group of SASW surface testing locations.

improvement is shown by the dashed green line in Figure 2a which involved extending the peak force level from 1.3 to 0.7 Hz before the peak force begins to decrease with decreasing frequency. This improvement required modifying the operational configuration from the normal mode shown in Figure 6a to the modified shaking mode shown in Figure 7a. In this case, a reinforced concrete slab that was slightly embedded and was a little larger than the base plate of Liquidator was constructed at the site to be profiled. The purpose of this slab was to create a stable platform for the



(a) Liquidator shaking vertically in the normal mode of operation  
 (b) Typical profiling depths

Figure 6. SASW profiling with Liquidator in the normal operating mode at a greenfield site in Georgia, USA;  $V_S$  profiles averaged about 340-m deep at a site of stiff soil over rock.

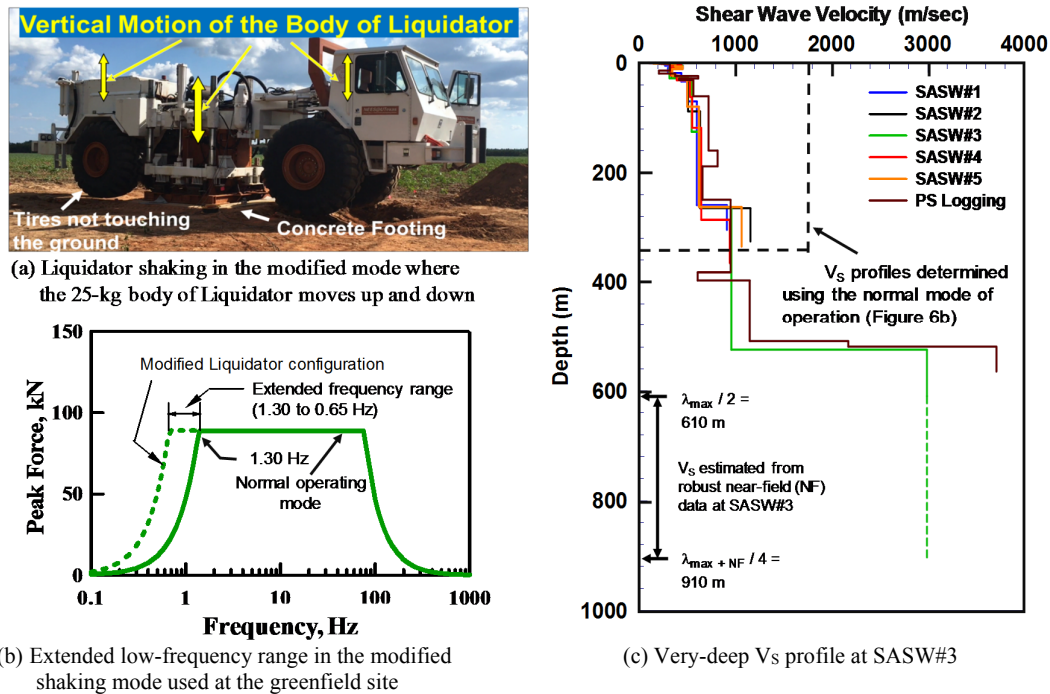


Figure 7. Active-source, very-deep  $V_s$  profiling with Liquidator shaking in the modified operational mode at a greenfield site in Georgia, USA.

base plate of Liquidator. The modified mode of operation was simply that the base plate of Liquidator remained stationary on the concrete slab while the flow of the hydraulic system was redirected so that the 25-kg “body of Liquidator” was lifted up and down, creating higher force levels at frequencies between about 1.30 to 0.65 Hz as shown in Figure 7b.

The modified mode of operation was first employed about three years ago at a “greenfield” site in Georgia, USA. A “greenfield” site is a possible location where new nuclear power plants may be constructed but the various required permits have not yet been submitted. Deep SASW testing was performed using the normal mode of operation at five locations around the greenfield site. The resulting VS profiles are presented in Figure 6b. In this case, deep VS profiling at the five locations averaged about 340 m. At one of the greenfield sites, designated as SASW#3, very deep (> 500 m) profiling using the modified operational mode was also performed. This very-deep profile is presented in Figure 7c and is shown in comparison to the other shallower profiles that are outlined by the dashed box. As seen in Figure 7c, the very-deep profiling depth using the normal data processing extended to 610 m and identified “bedrock” ( $V_s \sim 3000$  m/s) at a depth of about 525 m. However, this depth was extended to a depth of 910 m using robust near-field data over frequencies between 0.65 to 0.80 Hz.

### 3.4 Very-deep (> 500 m) profiling using combined active and passive surface-wave methods

Higher-than-expected, long-period ground motions induced by the Canterbury Earthquake Sequence of 2010-2011 could not be fully explained, and detailed back-analyses aimed at reproducing the recorded ground motions were hampered by the lack of information on the  $V_s$  structure of the deep, interlayered sand and gravel deposits of the Canterbury basin. Therefore, confidence in predicting more robust, future design ground motions from forward-analyses was lacking. The unique equipment resources of NHERI@UTexas were mobilized to Christchurch with the goal of performing very-deep (> 500 m), noninvasive  $V_s$  profiling to aid in developing a 3D velocity

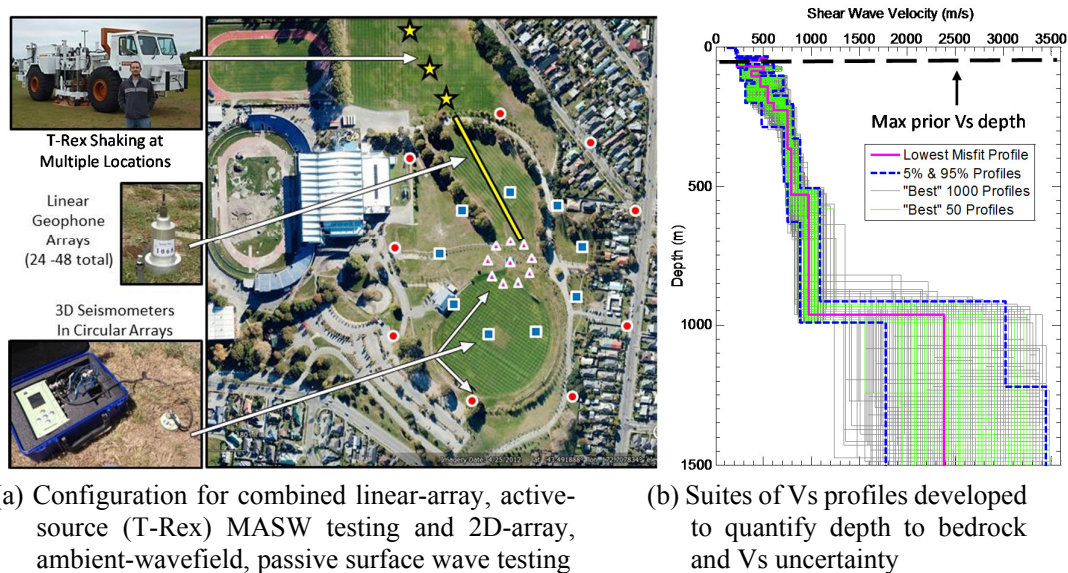


Figure 8. Active and passive, very-deep  $V_S$  profiling using surface waves in Christchurch, New Zealand.

model of the Canterbury basin (Thomson et al., 2019). The combined large, active-source and passive ambient-wavefield, surface-wave testing program had never before been applied. It involved deploying (see Figure 8a): (1) circular receiver arrays (up to 400 m in diameter) to record low-frequency ambient/microtremor waves with 120-s period Nanometrics seismometers, and (2) linear multi-channel-analysis-of-surface-waves (MASW) receiver arrays (up to 230-m long) to record waves generated actively with T-Rex. Extensive datasets were collected at 15 sites over a period of about 30 days. This unique equipment, coupled with advanced signal processing and data analysis techniques, allowed 500- to 1000-m deep  $V_S$  profiles to be developed at each site, with accompanying estimates of uncertainty (Teague et al., 2018). These  $V_S$  profiles revealed the subsurface structure, including a very strong, deep impedance contrast that played a significant role in the long-period amplification observed in the recorded ground motions. This information could not have been obtained economically in any other way. This project also highlights the shared-use facilities of NHERI@UTexas for a cooperative field study involving researchers from both countries.

#### 4 DEEP DOWNHOLE SEISMIC TESTING USING T-REX AS AN ACTIVE SOURCE FOR GENERATING CONTROLLED-WAVEFORM P AND S WAVES

Deep downhole seismic testing was employed to determine constrained compression-wave (P) and S-wave velocity profiles in two existing boreholes at the Los Alamos National Laboratory (LANL) in New Mexico, USA. Example measurements and results in the deeper borehole (415 m deep) are presented to illustrate the benefits of T-Rex as a powerful, hydraulically-controlled, waveform generator of P and S waves. In this borehole, traditional downhole testing with hand-operated impulsive sources was performed to determine P- and S-wave velocity profiles over the depth range of 18 to 183 m. Over depths from 153 to 415 m, T-Rex was used as the active source because it is capable of generating higher-energy waveforms for deeper profiling. An overlap zone in testing depths of 30 m with both types of seismic sources was used for comparison purposes and showed excellent agreement. In all measurements, a single, orientable, 3-D borehole geophone was used to monitor stress wave motions. Background information on the testing and analysis procedures are presented in Stokoe et al., 2017c. In this section, the general set-up with T-Rex as the seismic source, example P waveforms, a scaled waterfall plot of filtered P-wave

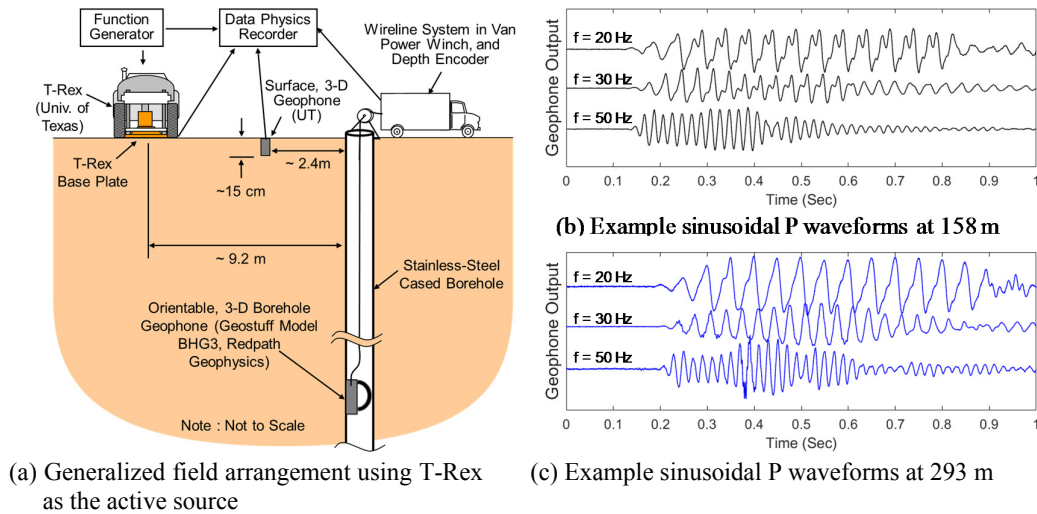


Figure 9. Arrangement for deep downhole testing at the Los Alamos National Laboratory using T-Rex as the active source to generate frequency-controlled, sinusoidal P and S waves at each testing depth (Stokoe et al., 2017c).

forms, and composite  $V_p$  and  $V_s$  profiles are presented. It is also worth noting that profiling could have continued well below 415 m if the borehole were deeper.

The generalized field arrangement using T-Rex as the active source is shown in Figure 9a. At each measurement depth, T-Rex was used to generate a controlled-waveform signal which in this project was a fixed-frequency signal that was composed of 10 full-amplitude cycles and 3 tapered-amplitude cycles at the beginning and end of the full-amplitude cycling. A frequency of 50 Hz was selected for most of the testing in the field to optimize the P and S waveforms. The selection process involved viewing the output waveforms from the borehole receiver at the start of data collection and at various depths during data collection. Examples of the variability in the sinusoidal P waveforms from T-Rex shaking at three different frequencies (50, 30 and 20 Hz) are presented in Figures 9b and 9c for depths of 158 and 293 m, respectively. As seen in Figure 9b, the simplest waveform to analyze at “shallow” depths was created by driving T-Rex with a 50-Hz signal. On the other hand, as the depth in the borehole increased, the clarity in the P waveform at lower frequencies improved as shown in Figure 9c, due mainly to longer wavelengths; hence, lower attenuation at deeper depths. In this case, the P-wave records are from a depth of 293 m, and both the 50- and 30-Hz records are clear. However, the 50-Hz measurements were continued to a depth of 360 m, below which depth the frequency was reduced to 30 Hz.

Waterfall plots of the filtered waveforms were used to determine consistent reference points with depth as shown in Figure 10a. It should be noted that the filtered waveforms in these plots were first scaled (amplified) according to depth squared before the reference points were picked. The first large peak in each scaled P waveform, identified as the borehole receiver point, Brp, is a surrogate for the P-wave arrival. The borehole reference points are identified by the red circles on the waveforms in Figure 10a. Once the Brps were picked, the times associated with the Brps were identified on the respective depth axes. These reference times are designated as borehole reference times, Brts, and are identified by the black circles on the depth axes in Figure 10a. The Brts were then used in waveform waterfall plots to initially identify zones of constant velocity. In this case, an initial linear regression line was fit to the data simply as a guide in identifying zones of constant velocity but realizing that actual velocities had to be evaluated from times of vertically propagating waves as discussed in Stokoe et al., 2017c.

Composite  $V_p$  and  $V_s$  profiles determined using the hand-operated and T-Rex sources are presented in Figure 10b. The geological profile at the borehole is shown in Figure 10c. The  $V_p$  and  $V_s$  profiles were divided into a common set of seven, constant-velocity layers. The velocity layering exhibited a general, but not perfect, correlation with the geological material profile, which is quite reasonable for these tuff materials. Values of Poisson’s ratio,  $\nu$ , were also calculated using

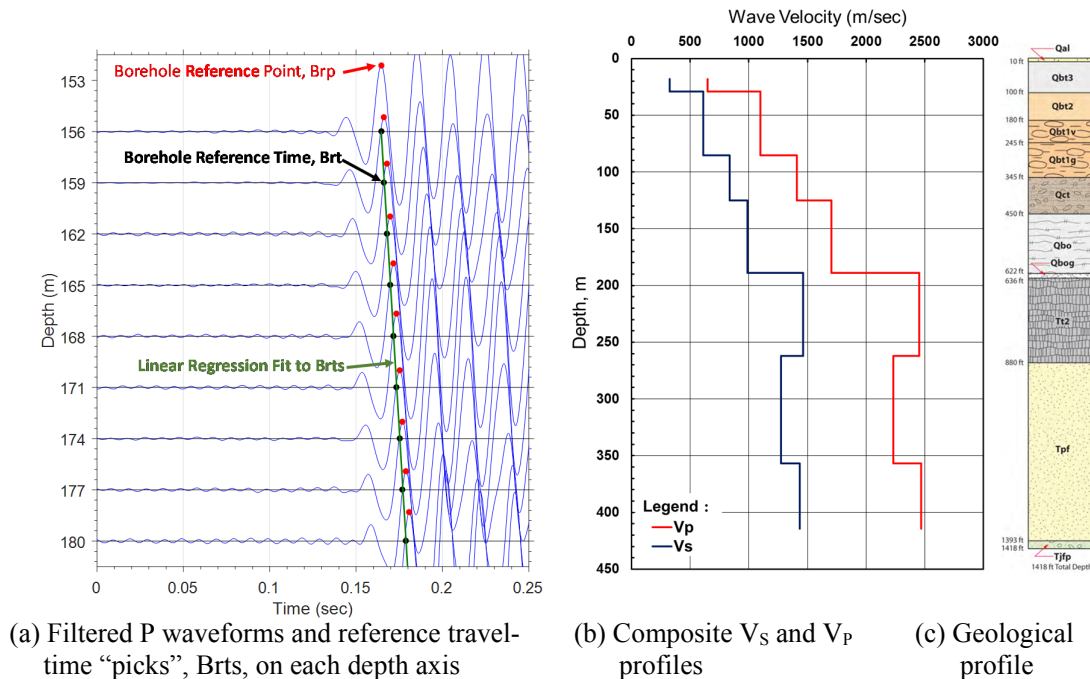


Figure 10. Example analysis of P waveforms to determine constant-velocity layers using T-Rex as the source, composite  $V_p$  and  $V_s$  profiles from hand-operated and frequency-controlled sources, and the site geological profile (Stokoe et al., 2017c).

the  $V_p$  and  $V_s$  profiles. The values of  $v$  ranged from 0.22 to 0.33. The highest values were in the shallowest geological layers. Once  $V_s \geq 835$  m/sec (at a depth  $\sim 85$  m), values of  $v$  ranged from 0.22 to 0.26. It should also be noted that wavelength,  $\lambda$ , is an important but overlooked variable in nearly all seismic measurements. In the case of body-wave measurements to determine the values of  $V_p$  and  $V_s$  in Figure 10b, it is important to consider two variables, the thickness of the layer and the length of each measurement interval compared with the wavelengths,  $\lambda_p$  and  $\lambda_s$ , respectively. In all of the measurements presented in Figure 10b, the wavelengths were longer the measurement interval. However, the P wavelengths are generally shorter than the thicknesses of the seven constant-velocity layers, and the S wavelengths are always shorter than the thicknesses of the seven constant-velocity layers in Figure 10b. The shortcoming in the conventional analysis procedure used in this downhole profiling occurred around the layer boundaries where a smearing of velocities occurs. On the other hand, the values in the central portion of each of the seven layers is correct. This topic is discussed in this conference (Hwang and Stokoe, 2019).

## 5 PARAMETRIC FIELD STUDIES OF LINEAR AND NONLINEAR STIFFNESSES

Parametric studies of geotechnical materials such as evaluating how  $V_s$  and  $V_p$  change with mean confining pressure ( $\sigma_0$ ) or how  $G$  varies with shear strain amplitude ( $\gamma$ ) are almost always performed in the laboratory. However, with the development of T-Rex and Thumper, these types of studies can now be conducted in the field. Over the past 15 years, such parametric studies have begun to be conducted. Initially, T-Rex and Thumper were used to develop a generalized staged-loading approach by which  $V_s - \log \sigma_0$ ,  $V_p - \log \sigma_0$  and  $G - \log \gamma$  relationships could be determined in situ. This type of parametric testing is needed because many geotechnical materials can not readily, or cost-effectively, be tested in the laboratory. These materials include: cemented alluvium, gravelly soils, loose gravelly, sandy and silty soils with or without plastic fines that are prone to liquefaction, and municipal solid waste. The generalized staged-testing approach involves creating an array of the appropriate sensors in the target material and shaking this material

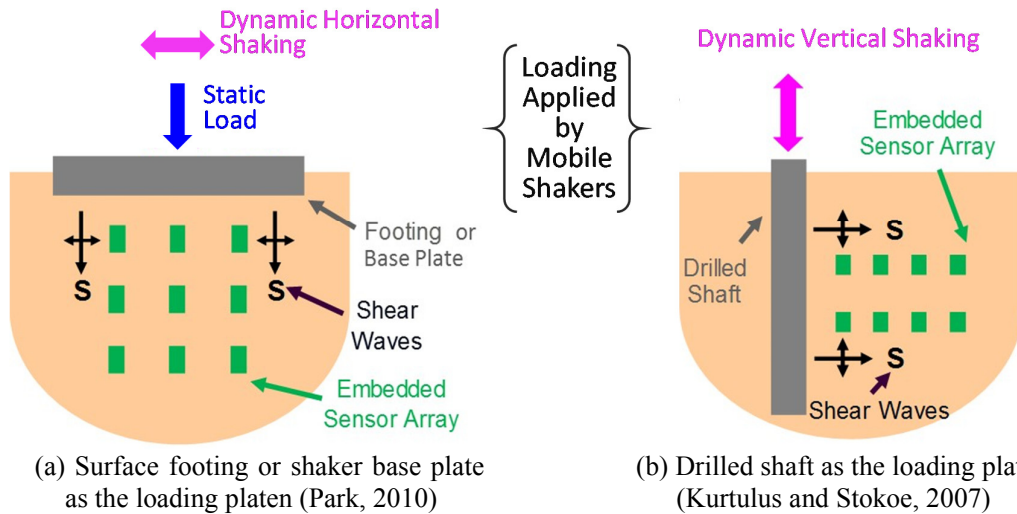


Figure 11. Next-generation field testing using frequency-controlled and load-controlled active sources for linear and nonlinear shear modulus measurements.

with some type of “controlled loading platen”. At this time, the loading platen at the ground surface has been either a concrete footing or the base plate of the mobile shaker (T-Rex or Thumper), as illustrated in Figure 11a (Park, 2010), while a reinforced-concrete, drilled shaft with a diameter of about 0.36 m has been used to excite deeper material, as illustrated in Figure 11b (Kurtulus and Stokoe, 2007).

One example that illustrates staged, dynamic testing of difficult-to-sample material is presented in Figure 12. These tests were conducted for use in the seismic design of the ground-level, waste-handling building at the proposed, geologic repository for high-level radioactive waste at Yucca Mountain, NV. The geotechnical material is a cemented alluvium which had never before been tested in situ to evaluate the  $G\text{-log } \gamma$  relationship. Concrete footings with a diameter of 0.91 m and an embedment of about 10 cm were constructed at three locations. These footings were used as loading platens for shear (S) wave excitation using Thumper (Figure 12a) and then T-Rex (Figure 12b) as the active sources. An embedded array of sensors, composed of 3D velocity transducers (geophones), was created beneath the concrete footings in a configuration similar to the array shown schematically in Figure 11a. The geophones were grouted in place in drilled boreholes using a weak grout. The results, in terms of  $G\text{-log } \gamma$ , are presented in Figure 13a. In this case, only

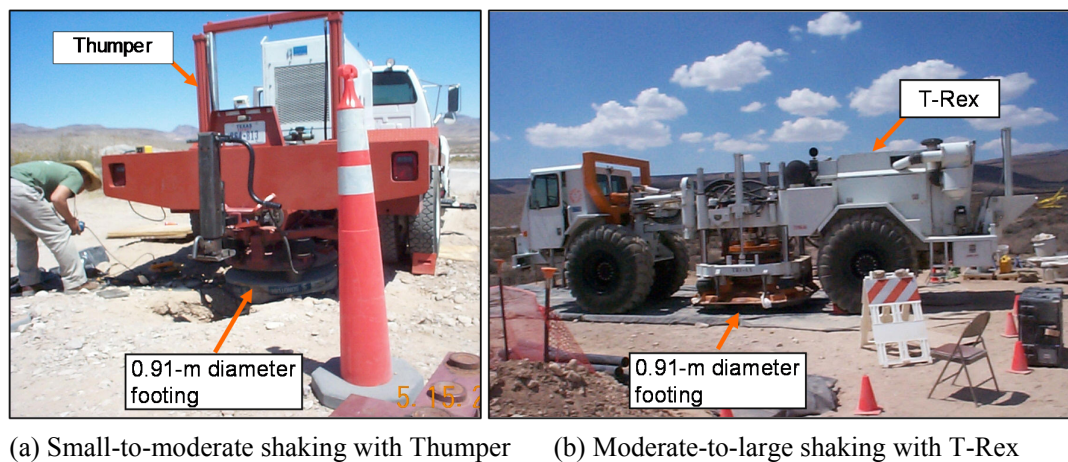


Figure 12. Linear and nonlinear steady-state dynamic testing of a cemented alluvium at Yucca Mountain (Park, 2010).

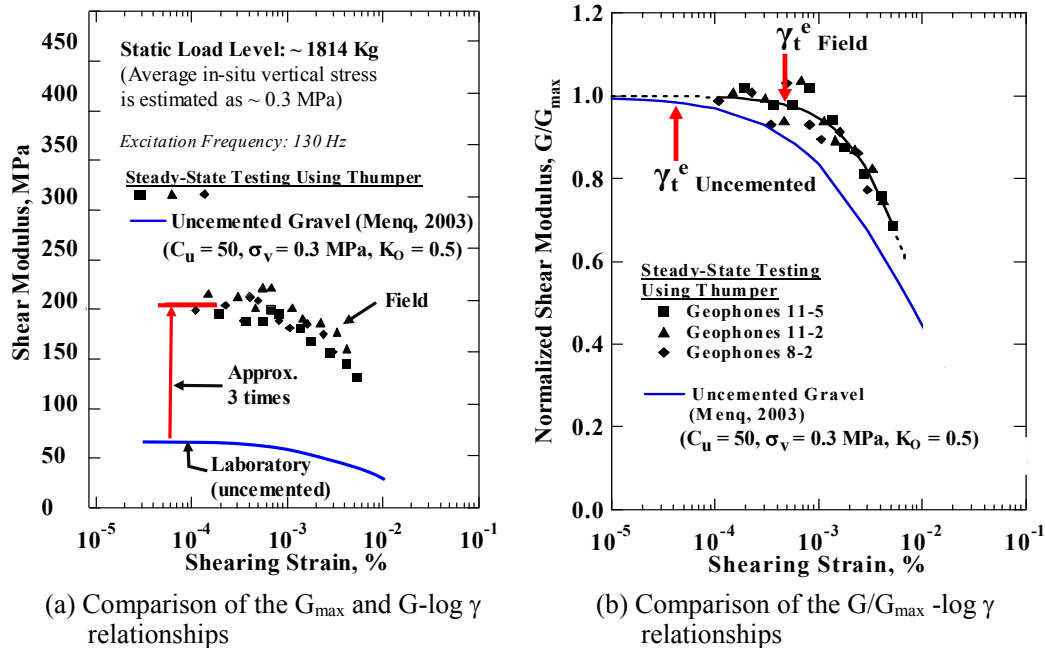
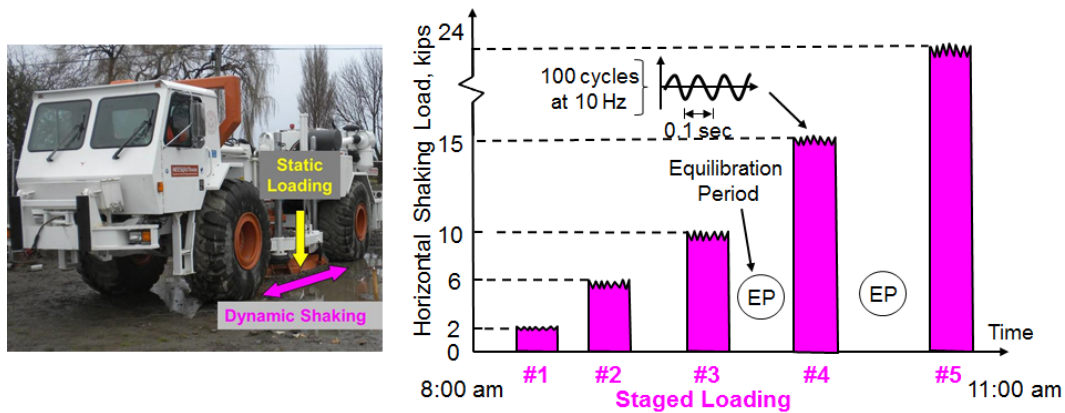


Figure 13. Comparisons of the  $G_{max}$  values,  $G$ - $\log \gamma$  relationships, and  $G/G_{max}$  - $\log \gamma$  relationships of cemented alluvium in the field and uncemented gravel in the laboratory.

Thumper was used as the active source. The results represent the first time that  $G$ - $\log \gamma$  data were determined in such a difficult material under controlled conditions. The in-situ measurements revealed that the cemented alluvium was approximately 3 times stiffer than would have been predicted by traditional, laboratory-based dynamic or cyclic methods with uncemented gravels (Menq, 2003). As noted in Figure 13a, the small-strain stiffness,  $G_{max}$ , is approximately three times greater in the cemented alluvium than in an uncemented gravel. As seen in Figure 13b, the elastic threshold strain  $\gamma_t^e$ , is about ten times larger and the nonlinearity increases more rapidly in the cemented alluvium compared to uncemented gravel. These findings are important and they were only possible because of the large, mobile hydraulic shakers. Other examples of this type of nonlinear testing include measurements of municipal solid waste (Stokoe et al., 2011 and Zekkos et al., 2014) and measurements of loose liquefiable sands that are discussed in Section 6.

## 6 IN-SITU LIQUEFACTION TESTING USING T-REX AS THE CONTROLLED SOURCE

With the development of T-Rex, the capability to apply large-amplitude, controlled-frequency, horizontal shaking in the field also offered researchers the opportunity to perform liquefaction studies in the field. Therefore, with T-Rex as a source, the methodology and general procedures for field liquefaction studies have been developed (Cox et al., 2009, Stokoe et al., 2014 and Roberts, 2017). As an example, liquefaction testing at a natural, sandy soil site in Christchurch, NZ is presented. This testing was performed about two years after the 2010-2011 Canterbury earthquakes that caused repeated, widespread and severe liquefaction throughout the suburbs of Christchurch. There was a serious need to investigate simple, cost-effective ground improvement methods to increase the resilience of residential construction during future earthquakes. As such, a series of full-scale field tests of various shallow ground improvement methods was initiated using T-Rex. Specifically, in-situ determinations of shear strain and excess pore-water pressure ratio ( $r_u$ ) during shaking were made in each of the four ground-improvement zones and two unimproved (natural soil) zones at three separate test areas around the city. T-Rex was used to perform staged loading directly on the ground surface (see Figure 14a) at all testing sites. A typical staged-loading sequence is presented in Figure 14b. The tendency for the ground improvement zones to strain



(a) T-Rex applying a vertical static load overnight followed by staged, horizontal shaking (b) Staged series of increasing horizontal shaking loads applied by T-Rex (A constant vertical load was continuously applied during shaking.)

Figure 14. Staged loading with T-Rex over a 24-hr period that included: (1) sensor installation, (2) an overnight consolidation process, and (3) staged loading at increasing horizontal shaking levels with T-Rex at six natural-soil test panels (Stokoe et al., 2014).

and buildup excess pore-water pressure under controlled shaking was evaluated relative to the natural-soil test panels. Example records at a depth of 2.1 m are presented in Figure 15 showing: (1) the build-up in excess pore-water pressure ratio ( $r_u = u_{\text{excess}}/\sigma'_v$ ) with number of cycles ( $N$ ) and, (2) the variation of shear strain ( $\gamma$ ) with number of cycles. The controlled sinusoidal loading was 10 Hz for 10 seconds. The response of the loose, saturated sand to 100 cycles of shaking at each stage in the five-staged loading sequence was determined.

The results from a complete set of staged loading tests of one natural-soil test panel are presented in Figure 16a in terms of  $r_u - \log \gamma$  for 30 cycles at each stage. Shear strains ranging from 0.0028% to 0.14% were generated in-situ. No measureable residual  $r_u$  was generated at cyclic shear strains less than 0.02%. At a threshold shear strain for pore-water pressure generation,  $\gamma_t^{PP}$ , of about 0.023%, residual excess pore-water pressure began to develop. As shear strain increased above  $\gamma_t^{PP}$ , the excess pore-water pressure began increasing more rapidly with each increasing

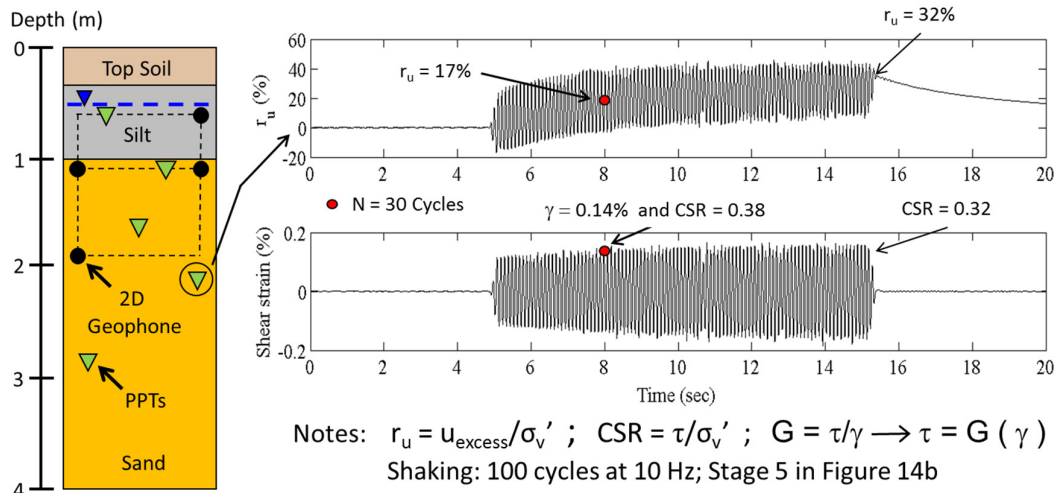


Figure 15. Liquefaction testing using T-Rex as the active source at one natural soil test panel in Christchurch, NZ; excess pore-water pressure ratio,  $r_u$ , versus time and shear strain,  $\gamma$ , versus time for 100 cycles of Stage 5 loading; note that values of  $r_u$ , and  $\gamma$  at 30 cycles of shaking are highlighted and used in Figure 16a.

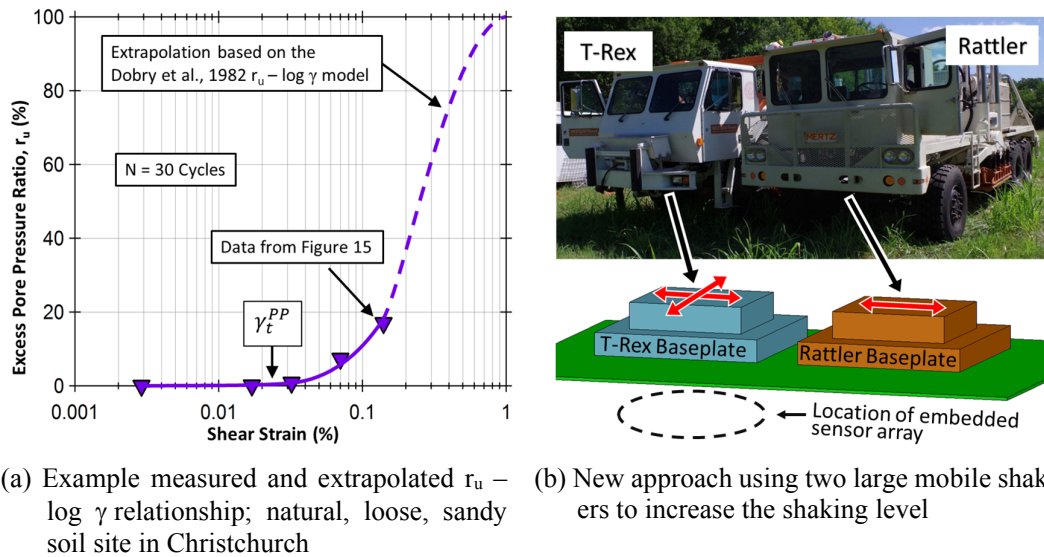


Figure 16. Example  $r_u - \log \gamma$  relationship estimated for the loose sands in Christchurch, NZ, and the new approach increasing the maximum strain during shaking

shear strain level. Unfortunately,  $r_u$  values above 17% for  $N = 30$  cycles could not be generated at this site. However, with the model of Dobry et al., 1982, the data were reasonably extrapolated to estimate the  $r_u - \log \gamma$  relationship of at least  $r_u \sim 80\%$ . To increase the shearing strains generated in future testing, the process of synchronizing two shakers in the field, as illustrated in Figure 16b, has been developed. This process will be used in Summer, 2019 in the Portland, Oregon area.

## 7 INVESTIGATING THE DYNAMIC AND SLOW-CYCLIC RESPONSES OF SCALED-STRUCTURAL SYSTEMS IN THE FIELD

In this example, three NHERI@UTexas shakers were involved in a collaborative effort to study soil-foundation-structure interaction in the field (Wood et al., 2004). This study was early in the development of the shakers and was performed shortly after T-Rex, Liquidator and Thumper were purchased. As a result, the work was performed under the NSF-sponsored NEES program, the predecessor to the NHERI program. All three shakers were used in testing two,  $1/4$ -scale, isolated bridge bents on drilled-shaft foundations that were constructed at a field site in Austin, TX. In this case, the mobile shakers offered researchers the advantage of studying soil-foundation-structure interaction of the scaled bridge bents under real conditions.

Each bridge bent was tested dynamically using five types of loading. Initially, the specimens were stuck with a modal hammer to generate the free-vibration response in the linear range of the complete system. In the second series of tests, T-Rex was used to induce sinusoidal motion in the test specimens by exciting the ground surface in the vertical and two horizontal directions. For the third series of tests, the shaker from Thumper was mounted at the midspan of the beam (see Figure 17a) and used to excite the bent horizontally, initially in the linear range and then in the nonlinear range. When the tests in this series were conducted using higher force levels, an inelastic response was observed. The structure would appear to have achieved resonance at a given excitation frequency. After a number of cycles with increasing response amplitude, the amplitude of the vibrations would decrease suddenly. This pattern was repeated several times during the stepped, sinusoidal-loading histories at higher force levels. No cracking of the concrete was observed after completion of these the tests. The decreasing natural frequency resulted from gaps that opened between the edges of the drilled shafts and the surrounding soil during the test series.

At the end of dynamic loading with Thumper, the wenches mounted in front of both T-Rex and Liquidator were used to slow cyclically load both of the bridge bents. Bridge Bent #2 is shown in

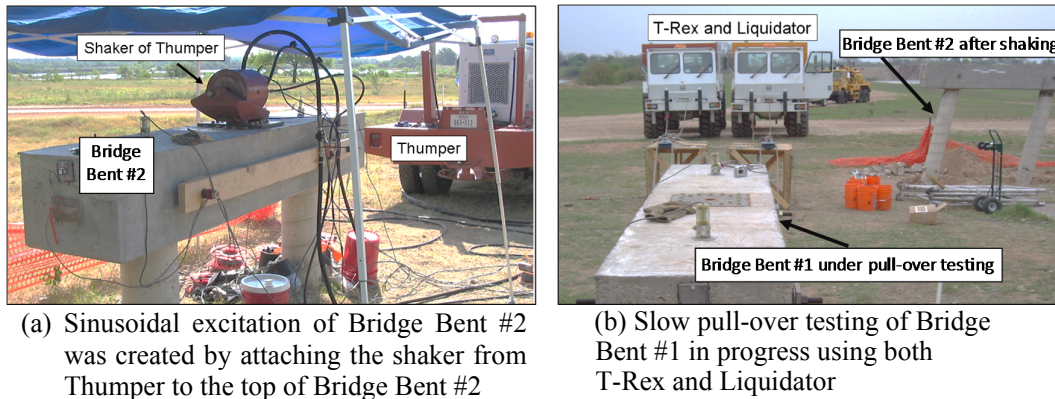


Figure 17. Dynamic, slow-cyclic and pull-over loading of two,  $\frac{1}{4}$  scale bridge bents in the field with the large mobile shakers

Figure 17b after the 2-way, slow cycling failed the two, column-shaft elements just below ground level. Bridge Bent #1 was not failed in the 2-way cyclic loading. Rather, it was failed in a one-way pull-over testing using T-Rex and Liquidator pulling together in Figure 17b.

## 8 CONCLUSIONS

The goal of this theme paper is to present examples of field testing, primarily in the geotechnical environment, that are now possible with the large mobile shakers of NHERI@UTexas and the shared-use policy of the U.S. National Science Foundation. The large mobile shakers can be used to apply all types of controlled dynamic loads on the ground surface or to structures embedded in the ground. Examples of deep to very deep (300 to 1000 m) surface-wave testing and deep down-hole measurements with P and S waves are presented. Parametric field studies such as evaluating the  $G - \log \gamma$  relationships of hard-to-sample materials and the generation of pore water pressure in loose sand (“liquefaction testing”) are also possible. The large mobile shakers can also be used to study the dynamic and slow-cyclic response of scaled-structures in the field. Hopefully, these examples have given the readers new and better ideas with which they can conduct research to improve our understanding of the natural and built environments.

## 9 ACKNOWLEDGMENTS

The authors would like to thank the U.S. National Science Foundation (NSF) for the financial support to develop and operate the NHERI@UTexas Equipment under grants CMS-0086605, CMS-0402490, and CMMI-1520808 and for the financial support for this research project under grants CMMI-1663654, CMMI-1663531, CMMI-1343524, CMMI 1303595, and NEESR 1041566. Special thanks also go to the staff at the University of Texas at Austin including Mr. Cecil Hoffpauir, Mr. Andrew Valentine and Mr. Robert Kent who assisted in the field work and Ms. Alicia Zapata for administrative assistance. There are also many other funding agencies that have supported these studies, many professional colleagues who have involved us in their projects, and numerous graduate students who have been involved. Unfortunately, space limitations of the paper do not permit specific thanks to be given to all of these organizations and individuals.

## REFERENCES

Cox, B.R., Stokoe II, K.H. and Rathje, E.M. 2009. An in-situ test method for evaluating the coupled pore pressure generation and nonlinear shear modulus behavior of liquefiable soils, *Geotechnical Testing Journal*, ASTM, 32(1).

- Dobry, R., Ladd, R., Yokel, F., Chung, R., and Powell, D. 1982. Predictions of pore water pressure buildup and liquefaction of sands during earthquakes by the cyclic strain method, *National Bureau of Standards, Building Science Series*, U.S. Department of Commerce
- Hwang, S., and Stokoe II, K.H. 2019. Comparison of downhole  $V_s$  profiles using conventional- and spectral- analysis methods, *7th International Conference on Earthquake Geotechnical Engineering*, Rome, Italy, June 17-20.
- Kurtulus, A., and Stokoe, II, K.H. 2007. Field method for measuring nonlinear soil behavior at depth using a dynamically loaded drill shaft. *Geotechnical Testing Journal*, ASTM, 26(4).
- Menq, F.-Y. 2003. Dynamic properties of sandy and gravelly soils. *Ph.D. Dissertation*, University of Texas at Austin.
- Natural Hazards Engineering Research Infrastructure (NHERI) 2017. Five-year science plan: multi-hazard research to make a more resilient world, <https://www.designsafe-ci.org/community/news/2017/nheri-science-plan-published-july-2017/>.
- Park, K., 2010. Field measurements of linear and nonlinear shear moduli of cemented alluvium using dynamically loaded surface footings, *Ph.D. Dissertation*, University of Texas at Austin.
- Roberts, J.N. 2017. Field Evaluation of Large-scale, shallow ground improvements to mitigate liquefaction triggering. *Ph.D. Dissertation*, University of Texas at Austin.
- Stokoe, K.H. II, Cox, B.R., and Menq, F.M., 2017a. NHERI@UTEXAS experimental facility: large-scale mobile shakers for natural-hazards field studies. *16th World Conference on Earthquake Engineering*, Santiago, Chile, January 9-13.
- Stokoe, K.H. II, Hwang, S., and Joh, S.-H., 2017b. Spectral-Analysis-of-Surface-Waves (SASW) testing to evaluate  $V_s$  profiles at geotechnical and geological sites. *16th World Conference on Earthquake Engineering*. Santiago, Chile, January.
- Stokoe, K.H. II, Hwang, S, Roberts, J.N., Menq, F.M., Keene, A.K., Lee, R.C and Redpath B 2017c. Deep downhole seismic testing using a hydraulically-operated, controlled-waveform vibroseis. *16th World Conference on Earthquake Engineering*. Santiago, Chile, January.
- Stokoe, II, K.H., Roberts, J.N., Hwang, S., Cox, B.R., Menq, F.Y. and Van Ballegooy, S, 2014. Effectiveness of inhibiting liquefaction triggering by shallow ground improvement methods: initial field shaking trials with T- Rex at one site in Christchurch, New Zealand. Orense, Towhata & Chouw (Eds.) *Soil liquefaction during recent large-scale earthquakes*, © 2014 Taylor & Francis Group, London, ISBN 978-1-138-02643-8
- Stokoe, II, K.H., Rosenblad, B.L., Wong, I.G., Bay, J.A., Thomas, P.A., and Silva, W.J., 2004. Deep profiling along the top of Yucca Mountain using a vibroseis source and surface waves. *Proceedings, 13th World conf. on earthquake. engineering*, Vancouver, Canada, August. Taylor & Francis Group, London, ISBN 978-1-138-02643-8.
- Stokoe II, K.H., Zalachoris, G., Cox, B.R., Park, K. 2011. Field evaluations of the effects of stress state, strain amplitude and pore pressure generation on shear moduli of geotechnical and MSW materials. *Proceedings, 5th International symposium on deformation characteristics of geo-materials (IS-Seoul)*, Korea.
- Teague, D.P., Cox, B.R., Bradley, B., Wotherspoon, L. 2018. Development of deep shear wave velocity profiles with estimates of uncertainty in the complex inter-bedded geology of Christchurch, New Zealand. *Earthquake spectra*. (<https://doi.org/10.1193/041117EQS069M>).
- Thomson, E.M., Bradley, B.A., Lee, R.L., Wotherspoon, L.M., Wood, C.M., Cox, B.R. 2019 submitted. Generalized parametric functions and spatial correlations for seismic velocities in the Canterbury, New Zealand region from surface-wave-based site characterization. *Soil dynamics and earthquake engineering*, submitted 18 December 2018, in review.
- Wood, S.L., Anagnos, T., Arduino, P., Eberhard, M.O., Fenves, G.L., Finholt, T.A., Futrelle, J.M., Grant, S.K., Jeremic, B., Kramer, S.L., Kutter, B.L., Matamoros, A.B., McMullin, K.M., Ramirez, J.A., Rathje, E.M., Saiidi, M., Sanders, D.H., Stokoe, K.H., & Wilson, D.W. 2004. Using NEES to investigate soil-foundation-structure interaction. *Proceedings, 13th world conference on earthquake engineering*, Vancouver.
- Zekkos, D., Sahadewa, A., Woods, R. D., and Stokoe, K., II 2014. Development of a model for shear wave velocity of municipal solid waste. *Journal of Geotechnical and Geoenvironmental Engineering*, ASCE, Vol. 140(3), March.